The Journal of Engineering and Exact Sciences – jCEC, Vol. 08 N. 06 (2022)
journal homepage: https://periodicos.ufv.br/jcec
eISSN: 2527-1075
ISSN: 2446-9416

Selective union of ATP vs ADP to an amino/amide macrocycle and its Cu^{2+} complexes: potentiometric, spectrophotometric and theoretical approximations

Fijación selectiva de ATP vs ADP a un macrociclo amino/amida y sus complejos Cu^{2+}: enfoques potenciométrico, espectrofotométrico y teórico

União seletiva de ATP vs ADP a um macrociclo de amino/amida e seus complexos Cu^{2+}: aproximações potenciométricas, espectrofotométricas e teóricas

Article Info:
Article history: Received 2022-05-20 / Accepted 2022-08-16 / Available online 2022-08-17
doi: 10.18540/jcecvl8iss6pp14571-01i

Armando Ferrer Serrano
ORCID: https://orcid.org/0000-0002-6849-0232
Departamento de Química, Facultad de Ciencias Naturales y Exactas, Universidad de Oriente, Cuba
E-mail: aferrer@uo.edu.cu
Yennys Hernández Molina
ORCID: https://orcid.org/0000-0002-1186-6120
Departamento de Química, Facultad de Ciencias Naturales y Exactas, Universidad de Oriente, Cuba
E-mail: yhmolina@uo.edu.cu

Abstract

The protonation equilibria of a new amine/amide type macrocycle and its complexation with Cu(II) in solution have been studied by potentiometry and UV-Visible Spectrophotometry. The ligand shows four protonation constants and one unusual deprotonation constant. Six mononuclear and four binuclear copper II complexes were found and reported its stability constant values. Some species predominate in specific ranges of pH, which might be important for biomimetic studies. It was found that the studied ligand forms stable mononuclear and binuclear complexes with Cu (II) and these species have similar geometries, squared pyramid, above pH 7. An evaluation through its potentiometrically determined stability constants of the selective recognition of ATP over ADP by this macrocycle and its Cu (II) complexes is presented. With or without the presence of Cu (II) ions, the ligand forms more stable complexes with ATP over ADP, the stability of these species increase with pH. Both, the stability quotients and the species distribution diagrams for the ATP-ADP mixed systems shows the inclination of the studied systems to selectively bind ATP over ADP, so, in principle, they can be used for the selective recognition of ATP or as catalysts in the hydrolysis of this nucleotide.

Keywords: Protonation. Copper complex. Macrocycle. ATP. ADP. Recognition. Selectivity quotient.

Resumen

Los equilibrios de protonación de un nuevo macrociclo de tipo amina/amida y su complejación con Cu(II) en solución han sido estudiados mediante potenciometría y espectrofotometría UV-Visible. El ligando muestra cuatro constantes de protonación y una constante de desprotonación inusual. Se encontraron seis complejos de cobre II mononucleares y cuatro binucleares y se reportaron sus valores constantes de estabilidad. Algunas especies predominan en rangos específicos de pH, lo que podría ser importante para los estudios biomiméticos. Se encontró que el ligando estudiado forma complejos mononucleares y binucleares estables con Cu (II) y estas especies tienen geometrías similares, pirámide cuadrada, por encima de pH 7. Una evaluación a través de sus constantes de estabilidad determinadas potenciométricamente del reconocimiento selectivo de ATP sobre ADP por este Se presenta el macrociclo y sus complejos de Cu (II). Con o sin la presencia de iones Cu(II), el ligando forma complejos más estables con ATP que con ADP, la estabilidad de estas especies aumenta con el pH. Tanto los cocientes de estabilidad como los diagramas de distribución de especies para los sistemas mixtos ATP-ADP muestran la inclinación de los sistemas estudiados a unir selectivamente ATP sobre ADP, por lo que, en principio, pueden ser utilizados para el reconocimiento selectivo de ATP o como catalizadores en la hidrólisis de este nucleótido.

Palabras-clave: Protonación. Complejo de cobre. Macrociclo. ATP. ADP. Reconocimiento. Cociente de selectividad.

Resumo

O equilíbrio de protonação de um novo macrociclo do tipo amina/amida e sua complexação com Cu(II) em solução foram estudados por potenciometria e espectrofotometria UV-Visível. O ligante mostra quatro constantes de protonação e uma constante de desprotonação incomum. Seis complexos mononucleares e quatro binucleares de cobre II foram encontrados e relataram seus valores constantes de estabilidade. Algumas espécies predominam em faixas específicas de pH, o que pode ser importante para estudos biomiméticos. Verificou-se que o ligante estudado forma complexos mononucleares e binucleares estáveis com Cu (II) e essas espécies possuem geometrias semelhantes, pirâmide quadrada, acima de pH 7. Uma avaliação através de suas constantes de estabilidade determinadas potenciométricas do reconhecimento seletivo de ATP sobre ADP por este macrociclo e seus complexos de Cu (II). Com ou sem a presença de íons Cu(II), o ligante forma complexos mais estáveis com ATP sobre ADP, a estabilidade dessas espécies aumenta com o pH. Tanto os quocientes de estabilidade quanto os diagramas de distribuição de espécies para os sistemas mistos ATP-ADP mostram a tendência dos sistemas estudados em ligar seletivamente ATP sobre ADP, portanto, em princípio, podem ser usados para o reconhecimento seletivo de ATP ou como catalisadores na hidrólise deste nucleótido.

Palavras-chave: Protonação. Complexo de cobre. Macrociclo. ATP – ADP. Reconhecimento. Quociente de seletividade.

Nomenclature

L: 2,16,22,36-tetraoxo-3,7,11,15,23,27,31,35-octazatriciclo[37.3.1.1^{17,21}]dotetraconta-1(41),17(42), 18,20,37,39-hexaeno.

1. Introduction.

Metalloenzymes usually contain metal ions bound to an amino group of a specific amino acid residue of a peptide or directly to the amide group –carbonyl or nitrogen– offering different coordination environments (Yang, 2022; Martell, 1995; Oloruntoyin, 2022). Thus, a proper de-sign of small molecules with suitable structural and func-tional characteristics could be important for future catalytic, biomimetic and recognition studies. In this regard, the design and synthesis of ligands functionalized to achieve metal complexation in a biomimetic approach is a challenge of current interest (Lehn, 1988; Jung, 2021; Bianchi, 1997). Amino/amide systems are able to dis-play interesting features, behaving as organogelators (Valls, 2022; Becerril, 2004; Rubio, 2013), acting as `in vivo´ fluorescent pH probes (Galindo, 2005), as selective receptors for substrates of biological relevance (Burguete, 2007), as mini-malistic molecular machines (Chao, 2009; Nazif, 2021), as ligands for the prepara-tion of enantioselective catalysts (Burguete, 2003) or as chiral solvating agents (Burguete, 2002). On the other hand, the self-assembly of this kind of compound in the solid state has also allowed the obser-vation of some remarkable crystalline structures and nano-assembled morphologies with relevance for the un-derstanding of structural parameters in proteins and related peptides' systems (Alfonso, 2009).

As an important part of biomimetic studies, the selective recognition of nucleotides is a crucial aspect of biological processes. Nucleotide recognition taking into account the existence of different structural components: nitrogen base (purine or pyrimidine), pentose and mainly, phosphate terminal chain. The bibliography describes a great variety of host created for selective adenosine phosphates recognition (Bazzicalupi, 2005; Nation, 1997; Reinke, 2021; Ciavardini, 2017), among the most common are polyamines (Aguilar, 2002; Bencini, 2014; Lomozik, 2005). Those systems are efficient, generally, due to the strong electro-static interactions between negative charged phosphates and protonates polyamines groups. In other hand, hydrogen bonds also may affect the stability and selectivity of the system host-guest (Cragg, 2010).

Recently, the synthesis, characterization and acidi-ty-basicity constants of a novel amino/amide type macro-cycle, named L (See Chart 1), have been published by the authors (Hernández, 2014). Here, the analysis of its binding ability towards a cation playing a key role in bioinorganic chemistry such as Cu (II) is presented, as well as the interaction with adenosine phosphates. The main variation considered has been the metal to ligand molar ratio, in order to analyze its effect on the coordination mode. ATP and ADP were studied with Cu (II) and the amino/amide macrocycle.

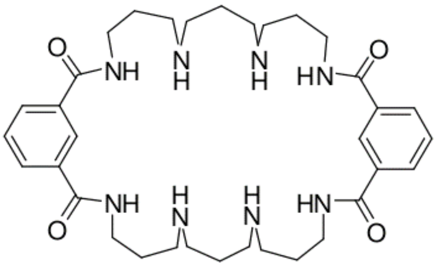

Chart 1 - Structure of the ligand L.

2. Materials and methods.

All reagents used in this work were purchased from commercial sources, except the isophthalic ester with N-hydroxysuccinimide, which was synthesized.

2.1 Synthesis of L.

The ligand L, used to perform the potentiometric measurements, was synthesized according to described procedures (Verdejo, 2007; Algarra, 2009). In a three-mouth ball, 100 mL of DME is added. Separately, in addition funnels, 0.29 mL (1.42 mmol) of N, N'- bis (3-aminopropyl) -1,3-diaminopropane are placed in one of them and in the other 0.50 g (1.39 mmol) of the isophthalic ester with N-hydroxysuccinimide previously synthesized (Both dissolved in DME). It is added dropwise into the receiving solvent placed on the balloon, under constant stirring and in an ice bath. The mixture is kept under stirring for 12 h, then the solid is removed by vacuum filtration, washed with DME and recrystallized from 2-propanol. Yield: 72 %; white solid; M.P: 131-132 ºC; HNMR (500MHz, DMSO-d6): δ(ppm) 8,67 (2H,s, Ar-H); 8,28 (4H,d, Ar-H); 7,93 (4H,s, amide); 7,51 (2H,s, Ar-H); 3,31 (8H,t, -CH_2-amide); 2,18-2,28 (4H,m,-NH-); 1,65 (8H,m, -CH_2-); 1,52 (4H,m, -CH_2-) ESI-MSMS (m/z,%): 638,4 (M + 2H+, 6); 419,4 (MW-218,2 +1,26); 368,3 ($C_{17}H_{30}N_5O_2^+$ + MeOH, 42), 335,3 ((M+ MeOH + 2H+)/2,19); 319,4 ((M + 2H+)/2, 11); 304,3 (MW-333,2 + 1, 100); 253,3 ((MW-132,02 + 3)/2, 88); Exp: C(63,23); N(18,34), H(8,56); Theo: C(64,12); N(17,60); H(8,23).

2.2 Potentiometric measurements.

The potentiometric titrations were carried out at 298.1 ± 0.1 K using NaCl 0.1 M as supporting electrolyte. The experimental procedure (burette, potentiometer, cell, stirrer, microcomputer, etc.) has been fully described elsewhere (Verdejo, 2007; Algarra, 2009). The acquisition of the emf data was performed with the computer program Crison Capture. The reference electrode was an Ag–AgCl electrode in saturated KCl solution. The glass electrode was calibrated as a hydrogen-ion concentration probe by titration of previously standardized amounts of HCl with CO_2-free NaOH solutions and the equiv. point determined by the Gran's method (Gran, 1952), which gives the standard potential, E°, and the ionic product of water [pKw = 13.78(1)]. The computer program HYPERQUAD (Gans, 1999) was used to calculate the protonation and stability constants, and the HySS program was used to obtain the distribution diagrams. The pH range investigated was 2.0–11.0 and the concentration of the metal ions and of the ligands ranged from 1 × 10–3 to 5 × 10–3 M with Cu^{2+}: L molar ratios as 1:1 and 2:1. In the case of ATP and ADP recognition studies were used an equivalent respect to the ligand L. The different titration curves for each system (at least two) were treated either as a single set or as separated curves without significant variations in the values of the stability constants. Finally, the sets of data were merged together and treated simultaneously to give the final stability constants. The electronic spectra were obtained in a Reyleigh UV-2601 Spectrophotometer.

3. Results and discussion.

3.1 Ligand protonation and Cu/L Systems.

The ligand presents four measurable protonation steps in the pH range of study. The first protonation constant coincides with the values reported for other secondary amines which suffer the effect of electro-withdrawing groups near them (Hernández, 2014; Alves de Silva, 2017). The decrease in the values of the successive protonation constants can be rationalized based on the electrostatic repulsion created by the consecutive addition of positive charges to the already positive charged specie.

The acidity constant obtained may be attributed either to the deprotonation of one of the amide nitrogen atoms or to the hydrolysis of one molecule of water bound by hydrogen bonds to both amide groups of one isophthalic moiety. The first of these options is less probable because the deprotonation of the amide group itself is a very endergonic process and can take place only if this negative contribution is more than compensated by a very exothermic interaction (Fabrizzi, 2008).

Table 1 – Logarithms of the cumulative and stepwise basicity and acidity constants determined in 0.1 M NaCl at 298.1 ± 0.1 K.

Species[a]	Log β	Equilibrium (K)	Log K
LH	9.41(5) [b]	[LH]/[L][H]	9.41(5)
LH_2	18.02(3)	$[LH_2]/[LH][H]$	8.61(3)
LH_3	25.37(5)	$[LH_3]/[LH_2][H]$	7.35(5)
LH_4	30.87(5)	$[LH_4]/[LH_3][H]$	5.50(5)
LH_{-1}	-9.64(5)	$[LH_{-1}]/[L][OH]$	-9.64(5)

[a] Charges omitted. [b] Values in parentheses are the error in the last significant figure.

The second option is supported by reports of crystalline structures of other compounds including isophtalic fragments, in which one molecule of water is attached by hydrogen bonds to both amide nitrogen atoms (Brooks, 2006; Bernier, 2009).

The corresponding species distribution diagram in 0.1 M NaCl is shown in Figure 1. It can be observed that below pH 5 the ligand is fully protonated, and that above pH 10, the deprotonated specie is predominant.

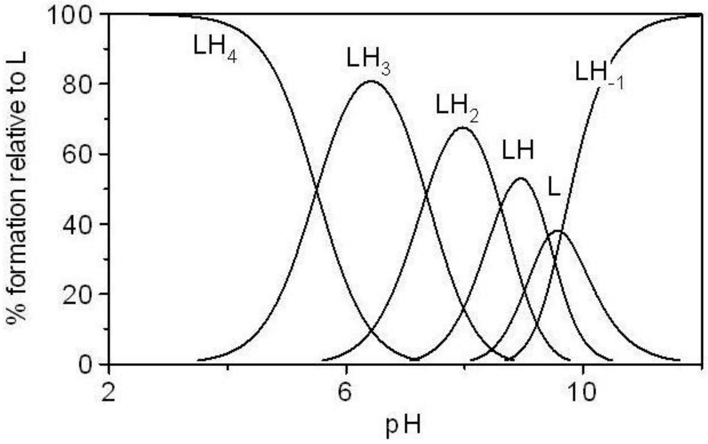

Figure 1 - Distribution diagram for the species of L in 0.1 M NaCl at 298.1 K.

Because of the interest of developing copper(II)-containing model systems for metalloproteins, the copper(II) complexes of the ligand was investigated to explore its coordination chemistry. The interaction of Cu^{2+} and the new ligand was systematically studied by potentiometric titrations in aqueous solution over the 2–12 pH range. The stability constants for the formation of Cu^{2+} complexes have been determined in water using 0.1 M NaCl to maintain a constant ionic strength and at 298.1 ± 0.1 K. The stability constants for Cu^{2+}:L ratio 1:1 are shown in Table 2. Six species of general formula $[CuLH_n]^{(2+n)+}$, where n = 3, 2, 1, 0, –1 and –2, were determined. Three of them were protonated. The CuL specie is more stable than the Cu(II) complex of 1,3-diaminepropane (tn) (See Chart 2) in molar ratio 1:1 (log K = 9.85),[24] but it is less stable than the complex specie $[Cu(tn)_2]^{2+}$ (log K = 17.45). On the other hand, the stability of CuL specie is similar, even higher, to those determined for other amine/amide compounds, in which the metal is bound to two amine groups and two amide oxygen. Considering this, although it cannot be stated, it cannot be discounted either the possibility that, for CuL specie, the copper ion has the coordination environment mentioned above. The species distribution diagram for this system is shown in Figure 2.

As it can be seen, the mononuclear specie is predominant at pH 7.12. The rest of the species do not exceed 70 % of relative abundance, although $CuLH_2$ is the major specie in the acid region and $CuLH_{-2}$ predominates at pH values above 10. For Cu^{2+}:L ratio 2:1 were determined four species of general formula $[Cu_2LH_m]^{(2+m)+}$, where m = 2, 1, 0 and –2. The formation constants for this system are shown in Table 3. The value of the stability constant for the Cu_2L specie is relatively low when compared with the value of the constant obtained for the ligand p-B232, in which every metal ion only can be bonded to two nitrogen atoms (See Chart 2). Also, the stability of this specie (log K = 17.61) is quite similar to the stability of the complex $Cu(tn)_2$ (log K = 17.45). Thus, it may be reasonable to propose that in this specie both copper ions have the same coordination environment than in the mononuclear specie.

Table 2 – Logarithms of the formation constants for the Cu^{2+} complexes of the ligand determined in 0.1 M NaCl at 298.1 ± 0.1 K at Cu^{2+}:L ratio 1:1.

Species[a]	Log β	Equilibrium (K)	Log K
$CuLH_3$	29.45(3) [b]	$[CuLH_3]/[CuLH_2][H]$	4.50(3)
$CuLH_2$	24.94(1)	$[CuLH_2]/[CuLH][H]$	5.70(1)
CuLH	19.24(2)	[CuLH]/[CuL][H]	6.21(2)
CuL	13.03(2)	[CuL]/[L][Cu]	-8.01(2)
$CuLH_{-1}$	5.02(2)	$[CuLH_{-1}]/[CuL][OH]$	-9.64(5)
$CuLH_{-2}$	-4.16(2)	$[CuLH_{-2}]/[CuLH_{-1}][OH]$	-9.19(2)

[a] Charges omitted. [b] Values in parentheses are the error in the last significant figure.

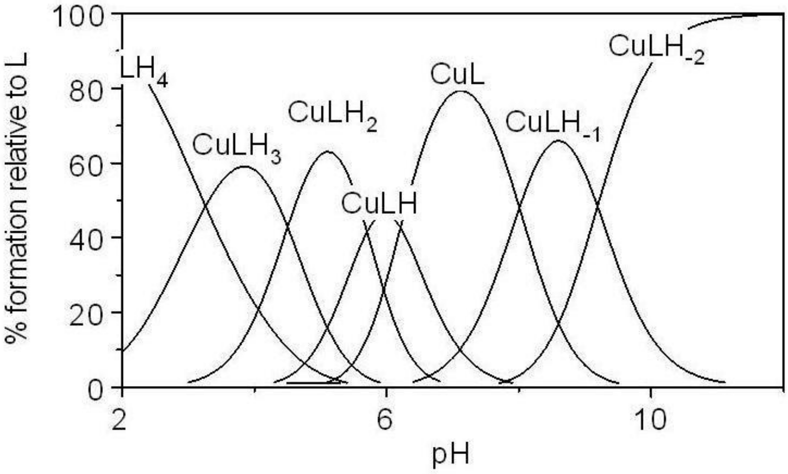

Figure 2 - Species distribution diagrams for the different Cu(II) complexes at Cu^{2+}:L ratio 1:1.

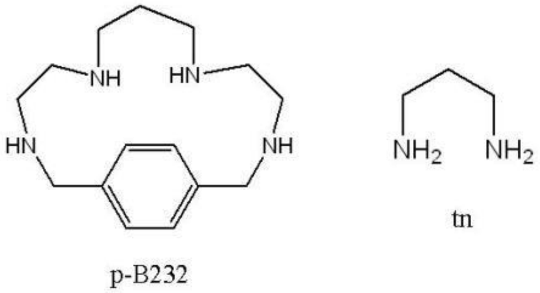

tn

p-B232

Chart 2.

Also, it can be observed the formation of the Cu_2LH_{-2} specie, which has a high stability and can be form by the simultaneous deprotonation of two amide nitrogen atoms, as literature suggests (Chao, 2009; Nazif, 2021; Martí, 2012). The species distribution diagram for this system is shown in Figure 3. It can be observed that the binuclear specie is predominant at pH 5.88. Also, Cu_2LH_{-2} specie is very stable and predominates in a wide range of pH, from 7.61 to 10.03.

Absorption spectra of Cu^{2+}–L systems in the 400-1000 nm region at different pH values and at different M:L molar ratios are shown in Figure 4. At pH approximately 3, both spectra have the same maximum (790 nm), which correspond to Cu^{2+} octahedral complexes. At this pH value, the predominant species are the aqueous Cu^{2+} complex ion and the $CuLH_3$ specie; which may have an octahedral geometry. Above pH 5, there are some differences between the spectra for both systems. For the Cu^{2+}–L system at 1:1 M:L molar ratio, at pH = 5.23, where $CuLH_2$ specie predominates, the absorption maxima is 730 nm, indicating a trigonal bipyramidal geometry. At pH values higher than 7, the absorption maxima ranges from 610 to 615 nm, suggesting that the coordination environment of the metal ion does not change substantially and could have a square pyramidal geometry. On the other hand, for the Cu^{2+}–L system at 2:1 M:L molar ratio, the maximum of the absorption peaks could not be determined for that region. Therefore, the interpretation of this spectrum becomes very difficult.

Figure 5 shows the absorption spectra of these systems in the 200-400 nm region at different pH values. For Cu^{2+}–L system at 1:1 M:L molar ratio, the bands associated with the $\pi\pi^*$ and $n\pi^*$ ligand transitions remains unchanged as the pH increases. Also, the charge transfer bands become more intense.

Table 3 – Logarithms of the formation constants for the Cu^{2+} complexes of the ligand determined in 0.1 M NaCl at 298.1 ± 0.1 K at Cu^{2+}:L ratio 2:1.

Species[a]	Log β	Equilibrium (K)	Log K
Cu_2LH_2	27.85(5) [b]	$[Cu_2LH_2]/[Cu_2LH][H]$	5.50(5)
Cu_2LH	22.36(10)	$[Cu_2LH]/[Cu_2L][H]$	4.75(10)
Cu_2L	17.61(3)	$[Cu_2L]/[CuL][Cu]$	4.58(3)
Cu_2LH_{-2}	4.75(3)	$[Cu_2LH_{-2}]/[Cu_2L][OH]^2$	-12.8(3)

[a] Charges omitted. [b] Values in parentheses are the error in the last significant figure.

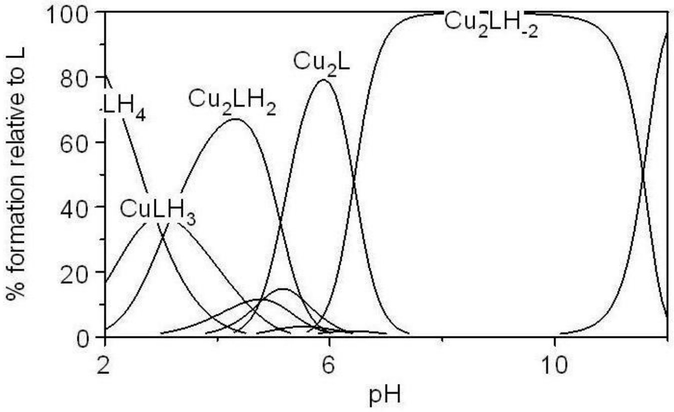

Figure 3 - Species distribution diagrams for the different Cu(II) complexes at Cu2+:L ratio 2:1.

On the other hand, for Cu^{2+}–L system at 2:1 M:L molar ratio, a substantial decrease in the intensity and change in the form of the $\pi\pi^*$ and $n\pi^*$ ligand transitions is observed at pH values between 5 and 7, as well as a significant increase of the intensity of the ligand-to-metal charge transfer bands as the pH increases. These two facts might be associated with Cu(II) coordination to deprotonated amide nitrogen atoms, which lead to a strong metal-ligand interaction and increase the intensity of the ligand-to-metal charge transfer bands (Inoue, 2001).

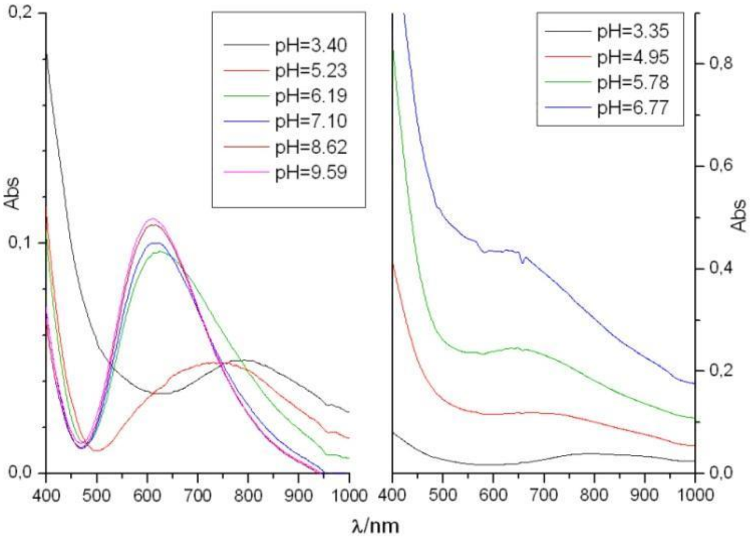

Figure 4 - Solution electronic spectra in the 400-1000 nm region for Cu^{2+}–L systems at different pH values and at different M:L molar ratios, 1:1 (left) and 2:1 (right).

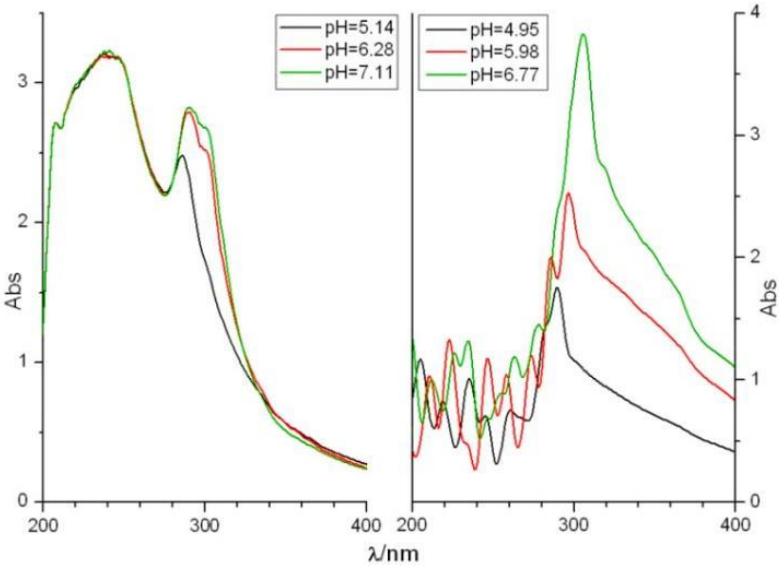

Figure 5 - Solution electronic spectra in the 200-400 nm region for Cu^{2+}–L systems at different pH values and at different M:L molar ratios, 1:1 (left) and 2:1 (right).

For Cu^{2+}–L system in this region of 200-500 nm with the molar ratio 1:1, bands associated with charge transfer are observed. At pH 5.14, where the specie $CuLH_2$ predominates, only one band centred at 286 nm is observed. From pH 6 when it begins the formation of the mononuclear specie CuL, this band is shifted to 290 nm and also appears a shoulder at 300 nm which could attribute that the metal is probably connected at two different ligand sites. If considering that the position of the maxima of charge transfer bands depend on donor electronegativity atom, it would prove that the hypothesis in those mononuclear species, Cu2+ ion is bonded to oxygen and amino nitrogen of the amide group.

At pH 9.28, where species $CuLH_{-1}$ and $CuLH_{-2}$ coexist, the charge transfer band maintains its absorption maximum at 290 nm with a shoulder at 303 nm, slightly increasing the intensity of the shoulder, which is consistent with the observed at lower pH values.

Interestingly, for the system Cu^{2+}–L in molar ratio 2: 1, the position of the charge transfer bands varies significantly with increasing pH. At pH 4.95, where the species Cu_2LH_2 (48%) predominates, the charge transfer band having a maximum at 290 nm with a shoulder at 282 nm. At pH 5.70, when the predominant species is Cu_2L (76%), two charge transfer bands, one centred at 285 nm and the other at 297 nm are observed, the latter being the most intense. At pH 6.77, in which the species Cu_2LH_{-2} has an abundance of 81%, the maximum charge transfer band is at 306 nm with a shoulder at 290 nm, this being very intense, suggesting that this species is formed by two deprotonated amide nitrogen.

3.2 ATP-ADP/L Systems.

The stability constants of this interesting system have been determined by potentiometric titrations (see Table 4). Three species were found for both systems, ADP-L and ATP-L 1:1 molar ratio. Generally, the nucleotide – ligand host-guest adduct are very stable if they are compared with other similar polyamines without amide groups (Guo, 2003; Ge, 2004; Bregier-Jarzebwska, 2019). In this study, ATP is the substrate best attached to the amino/amide ligand. It is possible to deduce that the link of both molecules (ATP and ligand) could be constituted mainly by hydrogen bonds of amidic groups as donators and phosphate oxygen as acceptors. Perhaps, adenine and pentose also could be involved in hydrogen interactions.

Table 4 – Logarithms of the stability constants for ATP/L and ADP/L complexes determined in 0.1 M NaCl at 298.1 ± 0.1 K at ratio 1:1.

Species[a]	Log β [b]		Equilibrium (K)	Log K	
	ATP	ADP		ATP	ADP
LAH_2	34.58(1)	31.54(1)	$[LAH_2]/[LH_2][A]$	16.56(1)	13.53(1)
LAH	31.07(4)	26.72(1)	[LAH]/[LH][A]	21.66(4)	17.32(1)
LA	28.27(1)	20.40(7)	[LA]/[L][A]	28.27(1)	20.40(7)

[a] Charges omitted. [b] Values in parentheses are the error in the last significant figure.

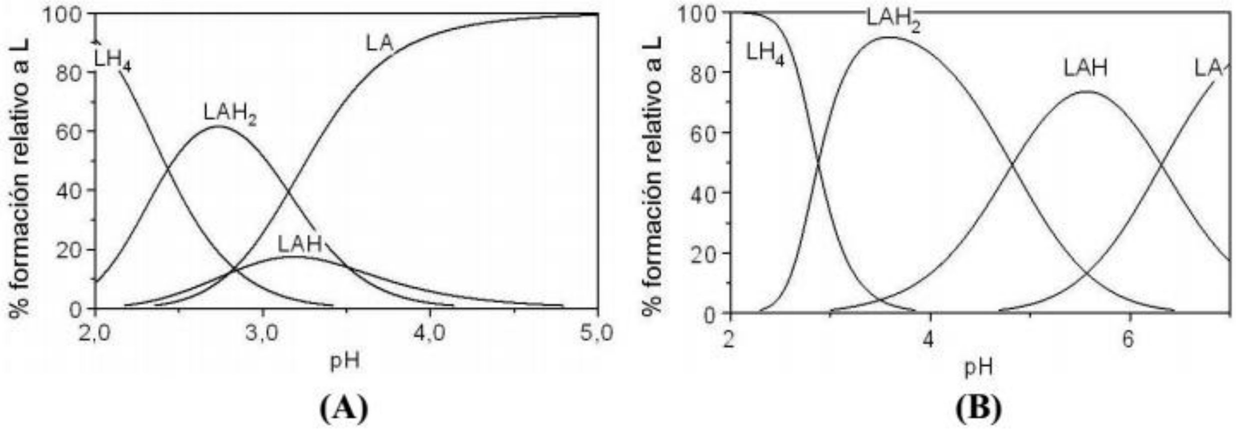

Figure 6 - Species distribution diagrams for the systems L/A (A=$ATP^{4–}$, $ADP^{3–}$), molar ratio L:A 1:1. (A) ATP y (B) ADP.

In other hand, the decreasing of the stability constant of the supramolecules respect to the increasing of protonation grade results particularly interesting. It is the opposite order that occurs for polyamine ligands (Burguete, 2007; Aguilar, 2002; Bencini, 2014; Lomozik, 2005). It is relevant to find LA species (A = ATP^{4-}, ADP^{3-}) with stability constant bigger than polyamine macrocycles tetraprotonated (Bencini, 2014; Lomozik, 2005).

Figure 6, shows the species distribution diagram for receptor-nucleotide system. For ATP is possible to observe a dominant specie LA, even at lower pH values; while for ADP the supramolecule LA only is abundant upper pH 6,5.

3.3 Cu^{2+}/ ATP-ADP/L Systems.

Stability constant for tertiary copper complexes with the main ligand and adenosine phosphates ATP and ADP were determined by potentiometric titrations. In all cases the molar ratio Cu:L:A was 1:1:1 and 2:1:1 (A = ATP^{4-}, ADP^{3-}), under the same conditions of the other systems already discussed in this paper. The results for the system 1:1:1 are shown in table 5.

Mononuclear complexes with this amino/amide ligand are able to joint ATP as well as ADP. Three complexes were found for ATP (one biprotonated and other triprotonated). While four species were determined for ADP (all protonated), with general formula $CuLADPH_n^{(n-1)+}$ (n = 2, 3, 4, 5). As we observed for ligand-nucleotide systems, the species with ATP are more stable than the ADP complexes, may be due to more electrostatic attractions and better possibilities of ATP to form Hydrogen bonds between host and guest.

Table 5 – Logarithms of the stability constants for Cu/ATP/L and Cu/ADP/L complexes determined in 0.1 M NaCl at 298.1 ± 0.1 K at ratio 1:1:1.

Species[a]	Log β [b]		Equilibrium (K)	Log K	
	ATP	ADP		ATP	ADP
$CuLAH_5$		45.27(1)	$[CuLAH_5]/[CuLAH_4][H]$		2.69(1)
$CuLAH_4$		42.58(1)	$[CuLAH_4]/[CuLAH_3][H]$		4.03(1)
$CuLAH_3$	41.67(3)[b]	38.55(1)	$[CuLAH_3]/[CuLAH_2][H]$	2.85(3)	4.22(1)
$CuLAH_2$	38.82(5)	34.33(3)	$[CuLAH_2]/[LAH_2][Cu]$	4.24(5)	2.78(3)
CuLA	32.58(2)		[CuLA]/[LA][Cu]	4.31(2)	

[a] Charges omitted. [b] Values in parentheses are the error in the last significant figure.

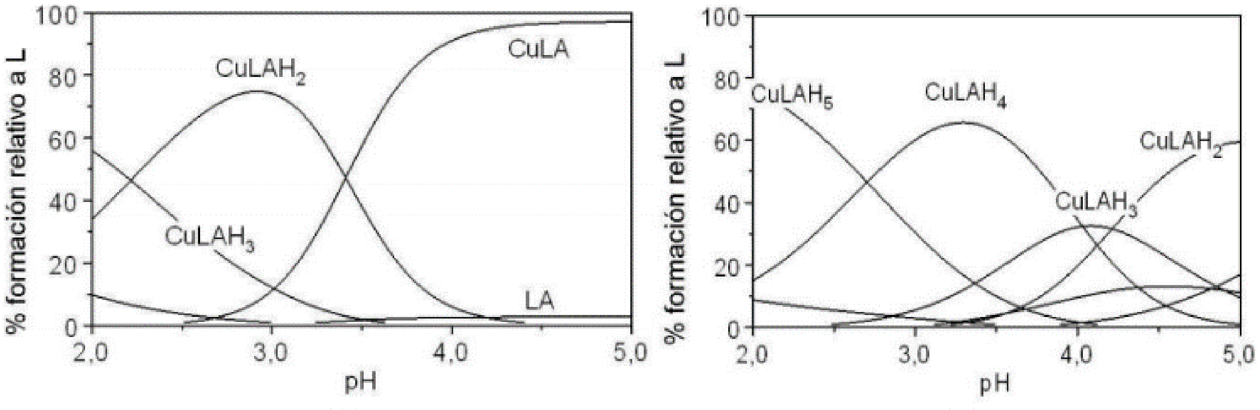

Figure 7 - Species distribution diagrams for the systems Cu(II)/L/A (A=ATP^{4-}, ADP^{3-}), molar ratio M:L:A 1:1:1. (A) ATP y (B) ADP.

Stability of specie LATP (log K = 28.27) is bigger than CuL (log K = 13.03). For this reason, it is possible to suppose that the specie CuLATP is the product of the Cu cation addition to the specie LATP (see Tables 4 and 5).

ATP can interact with amide groups by hydrogen bond, having free sites for cations. Cu^{2+} can link to ligand amine groups or ATP molecule as well, through free sites after ATP interact with the host. Following this idea, Cu^{2+} could be inside or out of macrocycle cavity having a different coordination environment respect to CuL. In fact, the stability constant for Cu^{2+} addition into the LATP adduct is relatively low (log K = 4.31), inferior to the CuATP complex formation constant (log K = 6.34).

In the other hand, if we compare the equilibrium constant for one Cu^{2+} incorporation to LAH_2, this process is more favorable for ATP than ADP. It is interesting that the entrance of one proton to $CuLAH_2$ is more favorable in the case of ADP respect to ATP. Maybe because in ATP this entrance could break a bond with bigger strength.

The Species Distribution Diagrams for ternary systems product of mononuclear complexes and nucleotides are shown in Figure 7. Correspondingly to the observation for L/A system, the non-protonated specie CuLATP at lower pH values is predominant, and can reach up to 95% of relative abundance. In the case of ADP, only the four protonated specie is clearly predominant, getting the 65.7% of relative abundance at pH 3.30.

Stability constant of ternary binuclear species of ATP and ADP with the amino/amide ligand and Cu^{2+} is shown in Table 6. Only one ATP binuclear complex was found, while three were determined for ADP. It is interesting that ATP binuclear complex shows more cumulative constant than the similar species with ADP. Also, if we check the values it is possible to think that the second Cu^{2+} entrance to $CuLAH_2$ is advantageous for the ATP ternary complex.

From the cumulative constant data for this system it was possible to build the species distribution diagram (Figure 8). This figure indicates that ATP ternary complex becomes significant from pH 2 until 5, where the ATP mononuclear copper complex appears. In the other hand, ADP complexes do not behave like ATP species in this case. There is not a clear possibility of isolation of one specie, coexisting one with others, although we can realize that binuclear species are predominant while pH increases. Cu_2LADPH_2 complex is the most abundant rising 51.8 % at pH 4.41.

Table 6 - Logarithms of the stability constants for Cu/ATP/L and Cu/ADP/L complexes determined in 0.1 M NaCl at 298.1 ± 0.1 K at ratio 2:1:1

Species[a]	**Log β** [b]		**Equilibrium (K)**	**Log K**	
	ATP	**ADP**		**ATP**	**ADP**
Cu_2LAH_3		41.11(3)	$[Cu_2LAH_3]/[Cu_2LAH_2][H]$		3.77(3)
			$[Cu_2LAH_3]/[CuLAH_3][Cu]$		2.56(3)
Cu_2LAH_2	43.52(3)[b]	37.34(2)	$[Cu_2LAH_2]/[Cu_2LAH][H]$		4.89(2)
			$[Cu_2LAH_2]/[CuLAH_2][Cu]$	4.70(2)	3.01(2)
Cu_2LAH		32.45(3)	$[Cu_2LAH]/[LAH][Cu]$		5.72(3)

[a] Charges omitted. [b] Values in parentheses are the error in the last significant figure.

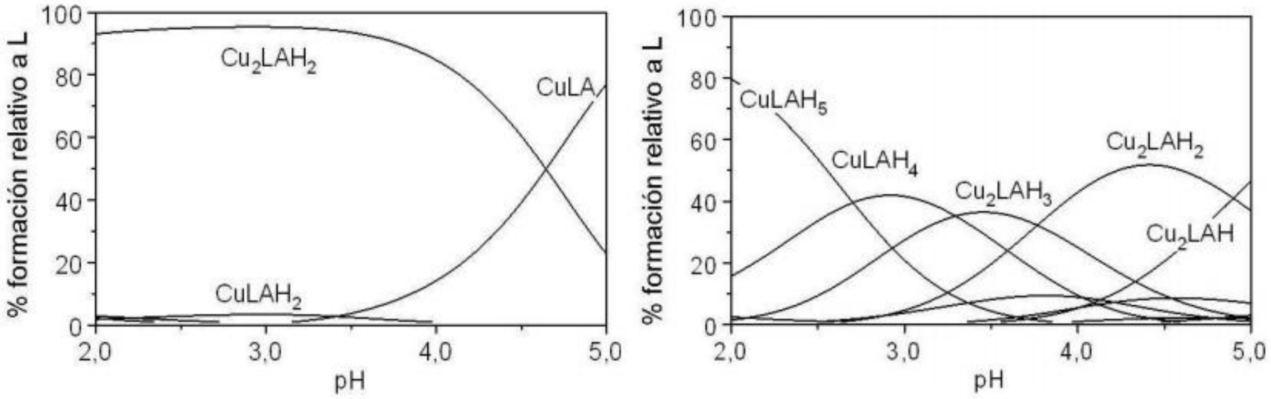

(A) **(B)**

Figure 8 - Species distribution diagrams for the systems Cu(II)/L/A (A=ATP^{4-}, ADP^{3-}), molar ratio M:L:A 2:1:1. (A) ATP y (B) ADP.

3.4 Selectivity of ligand and complexes for ATP respect to ADP.

Successful catalysis is based mainly in substrate recognition, selectivity and product release after chemical transformation. In aqueous solution, the host-guest complex stability is related to hydrogen bond formation, electrostatic interactions, as well as geometric “fit” of substrate into the receptor. In order to obtain a catalytic behavior a wanted characteristic is a strong union of substrate but a relatively weak union with the product. In this way, the last one can dissociate from resultant complex and continue the catalytic cycle (Lehn, 1988; Bianchi, 1997).

Usually, to express the selectivity relationship, quotients of stability constant are used (Bianchi, 1997). Then, for these systems, the selectivity relationship ATP/ADP for complex formation between the non-protonated ligand as receptor and both adenosine phosphates is 1.39. So, the receptor is selective to ATP respect to ADP and catalytic conversion ATP→ADP + Pi in amino/amide ligand could be reasonable. The product of the reaction, ADP, bonds the receptor less strongly than ATP, facilitating its release, even the catalytic conversion of ATP.

The selective relationships ATP/ADP for the species $CuLAH_2$ and Cu_2LAH_2 are 1.13 and 1.17, respectively. This analysis allows to think that for this ligand and its complexes ATP recognition is possible, including a possibility of a catalytic conversion into ADP. Logically, many studies must be done to apply it.

Nevertheless, for more complicated systems involving multiple protonation equilibria (receptor and anions) this simplification is impossible to support. It is necessary some criteria that balance the basicity differences with the aim of find selectivity patterns. There is a method to do it, by calculation of species distribution of receptor-anion1-anion2 combined systems and representing the percentage of total formation. The ATP-ADP combined system species distribution diagram for ligand and its mononuclear and binuclear complexes is shown in Figure 9. Is possible to note that the ATP species dominated all pH range vs ADP. There is a clear preference of ligand and complexes for ATP respect to ADP. In all cases, ADP species just reach 3% of relative abundance, suggesting that the inhibition of the reaction is not significant. It is clearly evident when is plotted the total percentage of the species in the ATP-ADP combined system (Figure 10). Initially, analyzing the ligand interacting with ATP and ADP simultaneously, is notable to observe that LATP at pH 2.5 have 70% of relative abundance and 100% is able at pH 4.5. The graph corresponding to the mixed copper-ligand-ATP-ADP system with a copper equivalent is shown in Figure 9B, where it is observed that the CuLATP species reach their highest relative abundance (> 80%) between pH 3.0 and 3.5, from pH 4.5 the abundance of these species begins to decrease significantly.

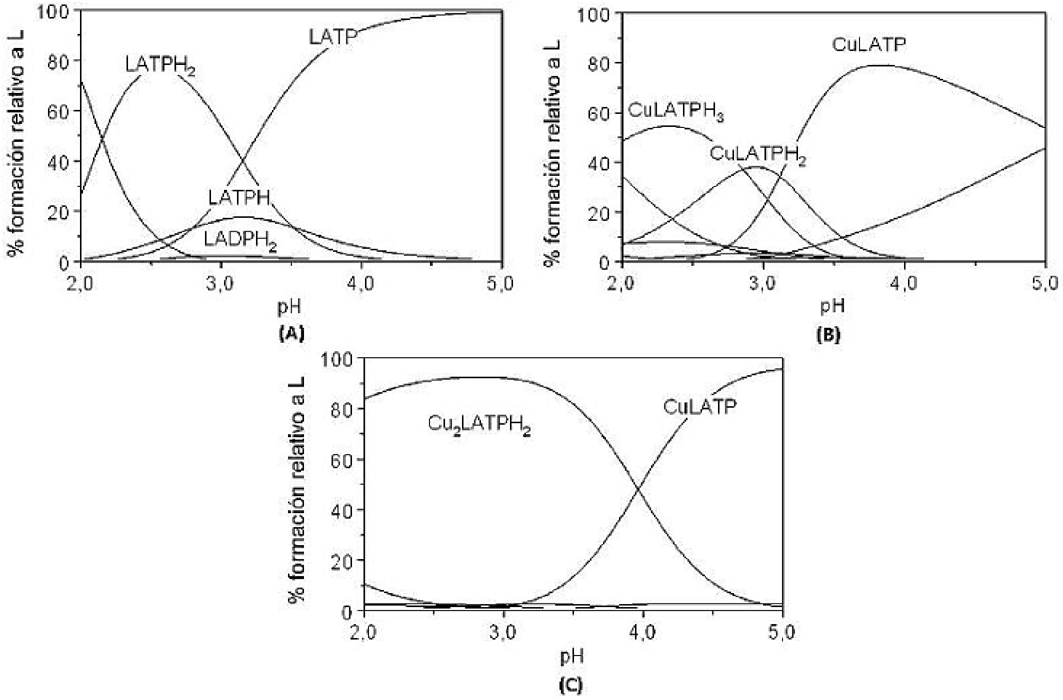

Figure 9 - Species distribution diagrams for the combined systems ATP–ADP (A) L/A, molar ratio 1:1, (B) Cu (II)/L/A, molar ratio 1:1:1 and (C) Cu (II)/L/A, molar ratio 2:1:1. (A=ATP^{4-}, ADP^{3-}).

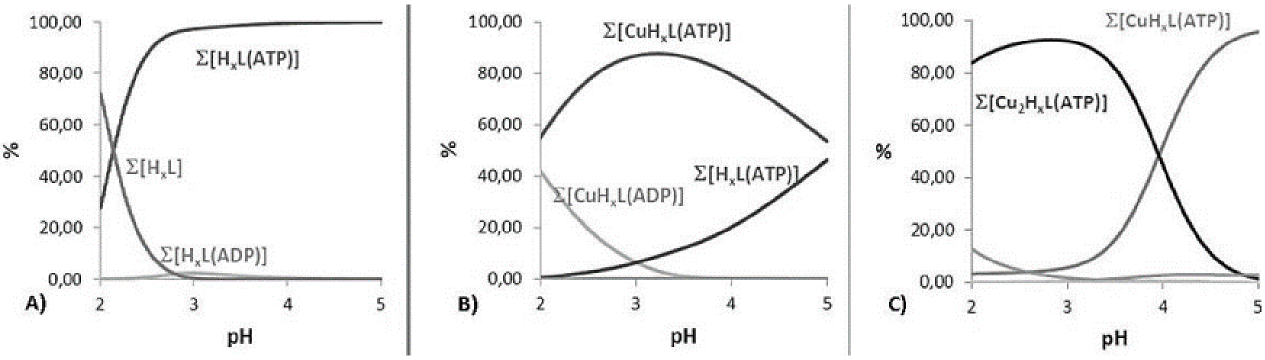

Figure 10 - Species distribution diagrams for total percentage of species vs pH for the combined systems ATP–ADP (A) L/A, molar ratio 1:1, (B) Cu (II)/L/A, molar ratio 1:1:1 and (C) Cu (II)/L/A, molar ratio 2:1:1. (A=ATP^{4-}, ADP^{3-}).

On the other hand, Figure 9C shows the total percentages of the species formed in the mixed copper-ligand-ATP-ADP system in the presence of two copper equivalents, it is observed that the Cu_2LATPH_2 species predominates below pH 3.5, between pH 3.5 and 4.5 coexist the Cu_2LATPH_2 and CuLATPHx species, from pH 4.5 the CuLATPHx species predominate. Comparing Figures 10B and 10C, we can see that an intensification in the concentration of Cu (II) increases the stability of the CuLATPHx species; thus, from pH 4.5, in the presence of an equivalent of copper the stability of these species begins to decrease, while in the presence of two equivalents of the metal they reach 86% abundance relative to said pH. Although there are other ATP recognition agent designs based on an uracil-linked hydroxyflavone (Botjar, 2018), this article was based on supramolecular interactions and may contain a possible ATP to ADP conversion reaction. Above all, it has focused on the development of molecular recognition in aqueous medium, inspired by cyclic pseudopeptide systems, such as those developed by Kubik and collaborators. (Kubik, 2017). Other authors have been developed similar systems by use of biogenic amines such as putrescine or spermidine, being a reference to compare results (Bregier-Jarzebwska, 2018).

3.5 Exploring supramolecular interactions by computational chemistry software: Spartan 08.

Spartan software is an interesting tool that shows 3D optimized structures and it helps to understand some aspects such as best conformations, macrocycle cavity size, energies, and also, spectra predictions (Omolara, 2018). Minimum energies of three types of different conformations of the ligand L were determined, considering that: a) the ligand was completely open (perhaps, occupying the cavity by water molecules); b) Intramolecular interactions between the amino and amide groups, leaving the aromatic rings in isolated positions; and c) that there are direct interactions between the aromatic rings. In the last two cases, the energies are very similar. However, when the macrocycle is fully open, the minimum energy is slightly higher. In any of the cases, the ligand L has the appropriate functional groups to attract, in a certain way, molecules that are also rich in electron-donating groups, as is the case with ATP.

Figure 11 shows such conformations as well as the energies of the supramolecular species formed between the amino/amide ligand and adenosine phosphates (ATP and ADP). Energetically, according to the results of Spartan 08, the values obtained are consistent with those obtained by potentiometric titrations, where more affinity of the ligand for ATP than for ADP is shown. It is possible to notice something interesting in this case, at least from a theoretical point of view. The energy of the supermolecule L+ATP is much lower than the homologue L+ADP; but the modes of interaction are not the same. L+ATP acquires an interaction called "perching" (outside interaction) described in bibliographies of supramolecular chemistry [32]; while L+ADP acquires a "nesting" type (interaction within the cavity). If the binding of ATP is thermodynamically more favored than that of ADP (according to the experimental values of Log K and the theoretically determined energies), we could potentially be in the presence of an ATP hydrolysis catalyst (Figure 12). However, this is not yet verifiable, as this reaction is still being studied by this team from the kinetic-mechanistic point of view.

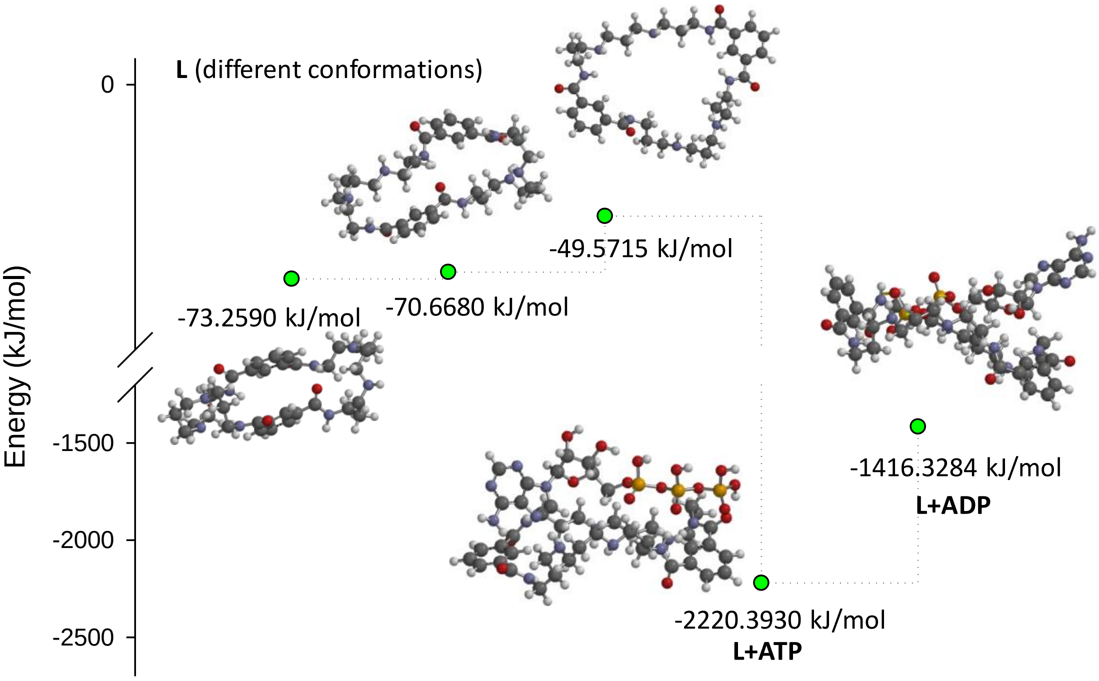

Figure 11 - Energetic diagram of L optimized by Spartan 08: L shows capacity of encapsulation of ATP (perching association, close but not inside the cavity) and ADP (nesting association, inside the cavity).

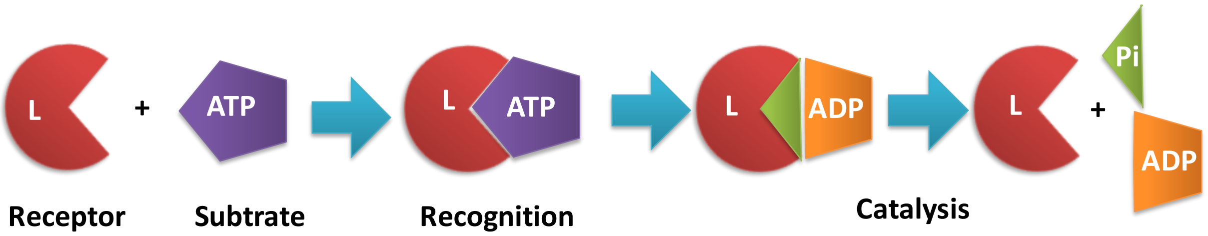

Figure 12 - Schematic representation of catalytic potential of L for ATP to ADP transformation.

Not only is stable the formation of ligand-adenosine phosphates supramolecules but also the metal complexes of copper II with this ligand, as well as the ternary species with adenosine phosphates. By molecular modelling in Spartan 08 was able to propose some structures based in direct interaction of ATP and ADP with binuclear complexes (Figure 13). There is a similar behavior respect to free ligand-adenosine phosphate interaction. Energies for both ternary complexes suggest a possible catalytic process.

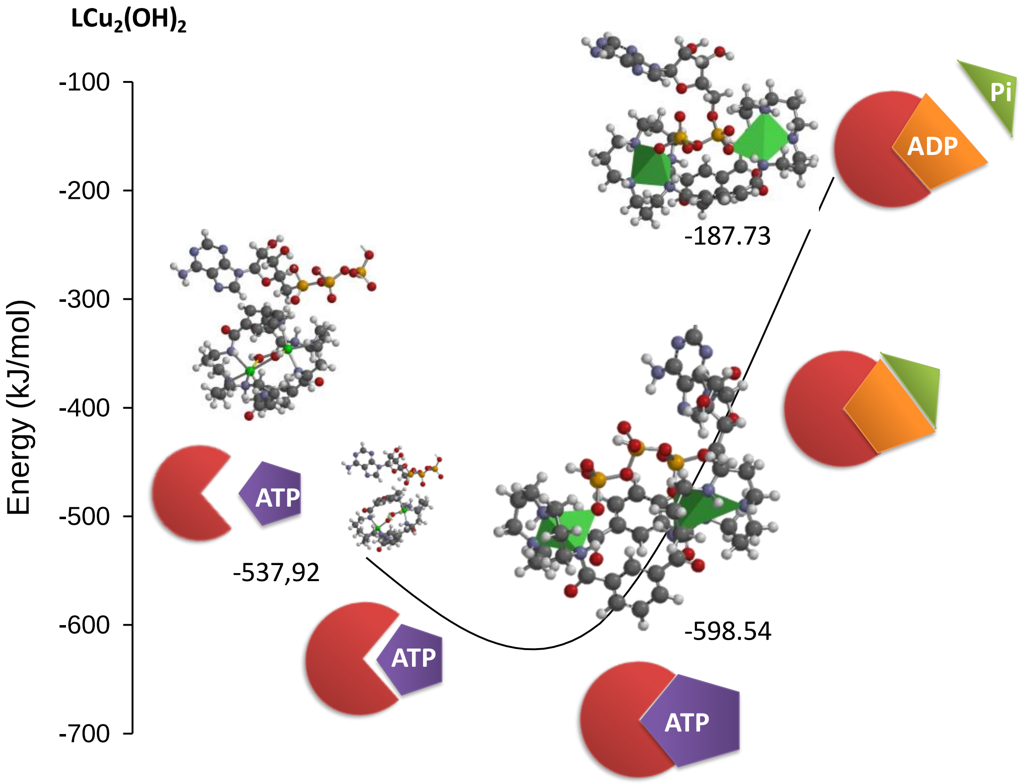

Figure 13 - Energetic diagram of binuclear complex LCu_2 interacting with ATP and ADP optimized by Spartan 08: clue for possible catalytic mechanism.

4. Conclusions.

In this work, it was shown that the ligand examined is able to form complexes of very different stoichiometry with Cu^{2+} depending on the metal to ligand ratio. Several pH-metric titrations have been conducted to analyze the complex formation. It is worth mentioning that two of the species determined predominates at physiological pH, which might be important for future biomimetic studies. The ligand forms mononuclear and binuclear stable complexes with Cu (II), showing by UV-visible spectroscopy that in general the species formed from pH 7 have similar geometries, of square-based pyramid. This amino/amide ligand forms more stable complexes with ATP than with ADP, also in the presence of Cu^{2+} ions, increasing the stability of these species as the pH increases. Both the stability quotients, and the species distribution diagrams for mixed ATP-ADP systems, show the inclination of the studied systems to selectively link to the ATP with respect to the ADP, so in principle they can be used for the selective recognition of the ATP or as catalysts in the hydrolysis of ATP.

Acknowledgements.

A. Ferrer wants to thank the Research Group Supramolecular and Sustainable Chemistry and Universitat Jaume I (Spain) for the financial support under the program "Plá de promoció de la investigació" and S. V. Luis, head of this group for the transmitted knowledge and friendship. Y. Hernandez-Molina thanks the financial support under "Ciencia y Conciencia" Project: "Syntheses of bioactive compounds designed by QSAR studies, using green chemical methods" by University of Oriente, Cuba.

References

Aguilar, J., Diaz, P., Escarti, F., García-España, E., Gil. L., Soriano, C., & Verdejo, B. (2002). Cation and anion recognition characteristics of open-chain polyamines containing ethylenic and propylenic chains., *Inorganica Chimica Acta*, 339, 307-316. https://doi.org/10.1016/S0020-1693(02)00947-7

Alfonso, I., Bolte, M., Bru, M., & Luis, S.V. (2009). Crystal structures of the HCl salts of pseudopeptidic macrocycles display "knobs into holes" hydrophobic interactions between aliphatic side chains. *Cryst. Eng. Comm.*, 11, 735. https://doi.org/10.1039/B821772F

Algarra, A., Basallote, M.G., Castillo, C.E., Clares, M.P., Ferrer, A., García-España, E., Llinares, J.M., Máñez, M.A., & Soriano, C. (2009). Geometric Isomerism in Pentacoordinate Cu^{2+} Complexes: Equilibrium, Kinetic, and Density Functional Theory Studies Reveal the Existence of Equilibrium between Square Pyramidal and Trigonal Bipyramidal Forms for a Tren-Derived Ligand., *Inorganic Chemistry*, 48, 902-914. https://doi.org/10.1021/ic8013078

Alves Da Silva, J., Felcman, J., Ramalho Mercê, A.L., Sálvio Mangrich, A., Lopes, R.S.C, & Cerqueira Lopes, C. (2003). Study of binary and ternary complexes of copper (II) with some polyamines and adenosine 5′ triphosphate., *Inorg. Chim. Acta*, 356, 155. https://doi.org/10.1016/S0020-1693(03)00462-6

Bazzicalupi, C., Bencini, A., Bianchi, A., Danesi, A., Giorgi, C., Lodeiro, C., Pina, F., Santarellia, S., & Valtancoli, B. (2005). A zinc(II)-based receptor for ATP binding and hydrolysis., *Chem. Commun.*, 630–2632. https://doi.org/10.1039/B502229K

Becerril, J., Burguete, M.I., Beatriu Escuder, B., Galindo, F., Gavara, R., Miravet, J.F., Luis, S.V., & Peris, G. (2004). Self-Assembly of Small Peptidomimetic Cyclophanes., **Chem. Eur. J.**, 10, 3879. https://doi.org/10.1002/chem.200400031

Bencini, A., Lippolis, V., & Valtancoli, B. (2014). Sensing and activation of anionic species by polyamine-based metal complexes., *Inorg. Chim. Acta*, 417, 38-58. https://doi.org/10.1016/j.ica.2014.01.003

Bernier, N., Carvalho, S., Li, F., Delgado, R., & Félix, V. (2009). Anion recognition by a macrobicycle based on a tetraoxadiaza macrocycle and an isophthalamide head unit., *J. Org. Chem.*, 74, 4819. https://doi.org/10.1021/jo9005798

Bianchi, A., Bowman-James, K., & García-España, E. (1997). *Supramolecular Chemistry of Anions*, Wiley-VCH, New York.

Bojtár, M., Zoltan, P., Mester, D., Hessz, D., Kállay, M., & Bitter, I., (2018). An uracil-linked hydroxyflavone probe for the recognition of ATP., *Beilstein J. Org. Chem.*, 14, 747-755. https://doi.org/10.3762/bjoc.14.63

Bregier-Jarzebwska, R., Łomozik, L. & Gąsowska, A., (2018). Influence of copper (II) ions on the noncovalent interactions between cytidine-5-diphosphate or cytidine-5′-triphosphate and biogenic amines putrescine or spermidine., *J. Inorg. Biochem*, 184, 27-33. https://doi.org/10.1016/j.jinorgbio.2018.04.003

Bregier-Jarzebwska, R., Stegient-Nowicka, J., Hoffmann, S. K., Gąsowska, A., & Łomozik, L. (2019). Studies of ternary complexes formed in the biocoordination systems including copper(II) ions, polyamines and L-lysine., *Polyhedron*, 173, 114137. https://doi.org/10.1016/j.poly.2019.114137

Brooks, S.J., Gale, P., & Light, M.E., (2006). Network formation by a pyrrole functionalized isophthalamide., *Cryst. Eng. Comm.*, 8, 877. https://doi.org/10.1039/B612524G

Burguete, M.I., Collado, M., Escorihuela, J., Galindo, F., García-Verdugo, E., Luis, S.V., & Vicent, M.J. (2003). Nickel complexes from α-amino amides as efficient catalysts for the enantioselective Et_2Zn addition to benzaldehyde. *Tetrahedron Letters*, 44, 6891. https://doi.org/10.1016/S0040-4039(03)01705-2

Burguete, M.I., Fréchet, J.M.J., García-Verdugo, E., Janco, M., Luis, S.V., Svec, F., Vicent, M.J., & Xu, M. (2002). New CSPs based on peptidomimetics: efficient chiral selectors in enantioselective separations., *Polymer Bulletin*, 48, 9. https://doi.org/10.1007/s00289-002-0005-3

Burguete, M.I., García-España, E., López-Diago, L., Luis, S.V., Miravet, J., & Sroczynski, D. (2007). Oxaaza cyclophanes in the recognition of nucleotides. The role of oxygen and electron-rich aromatic rings, *Org. Biomol. Chem.*, 5, 1935. https://doi.org/10.1039/B704305H

Ciavardini, A., Dalla, A., Fornarini, S., Scuderi, D., Giardini, A., Forte, G., Bodo, E., & Piccirillo, S. (2017). Adenosine monophosphate recognition by zinc–salophen complexes: IRMPD spectroscopy and quantum modeling study., *J. Mol. Spectroscopy*, 335, 108-116. https://doi.org/10.1016/j.jms.2017.02.014

Cragg, P.J., (2010). *Supramolecular Chemistry: From Biological inspiration to Biomedical applications*, Springer Dordrecht Heildelberg, London.

Chao, M-S., Lu, H-H., Tsai, M-L., Lin, Ch-M., & Hsieh, T-H. (2009). Molecular switching of nickel (II) complexes using a hemilabile N, N′-bis (β-carbamoylethyl) 1, 2-diaminocyclohexane ligand. *Inorg. Chem. Comm.*, 12, 1088. https://doi.org/10.1016/j.inoche.2009.08.025

Fabbizzi, L., (2008). Chapter: Fluorescent Sensors for and with Transition Metals, in *Transition Metals in Supramolecular Chemistry*, (Ed.: J. P. Sauvage), John Wiley & Sons, New York.

Galindo, F., Burguete, M.I., Vigara, L., Luis, S.V., Kabir, N., Gavrilovic, J., & Russell, D.A. (2005). Synthetic Macrocyclic Peptidomimetics as Tunable pH Probes for the Fluorescence Imaging of Acidic Organelles in Live Cells, *Angew. Chem. Int. Ed.*, 44, 6504. https://doi.org/10.1002/anie.200501920

Gans, P., Sabatini, A., & Vacca. A. (1996). Investigation of equilibria in solution. Determination of equilibrium constants with the HYPERQUAD suite of programs., *Talanta*, 43, 1739. https://doi.org/10.1016/0039-9140(96)01958-3

Ge, R., Lin, H., Xu, X., Sun, X., Lin, H., Zhu, S., Ji, B., Li, F., Wu, H. (2004). Catalysis of phosphoryl transfer from adenosine-5’-triphosphate (ATP) by trinuclear “chelate” complexes., *J. Inorg. Biochem.*, 98, 917-924. https://doi.org/10.1016/j.jinorgbio.2004.03.007

Gran, G., (1952). Determination of the Equivalence Point in Potentiometric Titrations. Part II., *Analyst*, 77, 661. https://doi.org/10.1039/AN9527700661

Guo, Y., Ge, Q., Lin, H., Lin, H. K., Zhu, S., & Zhou, C. (2003). The different roles of metal ions and water molecules in the recognition and catalyzed hydrolysis of ATP by phenanthrolinecontaining polyamines. *Biophysical Chemistry*, 105, 119-131. https://doi.org/10.1016/S0301-4622(03)00140-6

Hernández, Y., Ferrer, A., & Blanco, M. (2014). Nuevo macrociclo tipo amino/amida: síntesis, caracterización y constantes de acidez/ basicidad. *Revista Cubana de Química*, XXVI, 32. ISSN 2224-5421.

Inoue, M.B., Machi, L., .Muñoz, I. C., & Fernando, Q. (2001). Metal–ligand interactions in benzodioxotetraaza-macrocyclic metal chelates., *Inorg. Chim. Acta*, 324, 73-80. https://doi.org/10.1016/S0020-1693(01)00536-9

Jung, S-M., Lee, J., & Song, W-J. (2021). Design of artificial metalloenzymes with multiple inorganic elements: The more the merrier., *J. Inorg. Biochem.*, 223, 111552. https://doi.org/10.1016/j.jinorgbio.2021.111552

Kubik, S., (2017). Anion recognition in aqueous media by cyclopeptides and other synthetic receptors., *Acc. Chem. Res.*, 50(11), 2870-2878. https://doi.org/10.1021/acs.accounts.7b00458

Lehn, J. M. (1988). Supramolecular Chemistry—Scope and Perspectives Molecules, Supermolecules, and Molecular Devices (Nobel Lecture), *Angew. Chem. Int. Ed. Engl.*, 27, 89. https://doi.org/10.1002/anie.198800891

Lomozik, L., Gąsowska, A., Bregier-Jarzebwska, R., & Jastrza, R. (2005). Coordination chemistry of polyamines and their interactions in ternary systems including metal ions, nucleosides and nucleotides., *Coord. Chem. Rev.*,249, 2335-2350. http://doi.org/10.1016/j.ccr.2005.05.002

Martell, A., and Hancock, R. (1995). *Metal Complexes in Aqueous Solutions*, Plenum Press, New York.

Marti, I., Ferrer, A., Escorihuela, J., Burguete, M.I., & Luis, S.V. (2012). Copper (II) Complexes of Bis(amino amide) Ligands: Effect of Changes in the Amino Acid Residue, *Dalton Trans.*, 41, 6764. https://doi.org/10.1039/C2DT12459A

Nation, D.A., Lu, Q., & Martell, A. (1997). Molecular recognition of nucleotides by the protonated macrocyclic ligand 3,6,9,17,20,23-hexaazatricyclo[23.3.1.111,15]triaconta-1(29),11(30),12,14,25,27-hexaene and by its Cu(II) complexes; catalysis of the conversion of ATP to ADP., *Inorganica Chimica Acta*, 263, 209-217. https://doi.org/10.1016/S0020-1693(97)05699-5

Nazif, M., Sahin, E., & Erbas-Cakmak, S., (2021). Bio-inspired molecular machines and their biological applications. *Coord. Chem. Rev.*, 443, 214039. https://doi.org/10.1016/J.CCR.2021.214039

Oloruntoyin, Y., Adesina, W., Funmilayo, H., Olabisi, M., & Nizam, M., (2022). Metalloenzyme mimicry and modulation strategies to conquer antimicrobial resistance: Metal-ligand coordination perspectives., *Coord. Chem. Rev.*, 453, 214317. https://doi.org/10.1016/j.ccr.2021.214317

Omolara, A., (2018). Computational modelling Procedures for Geometry Optimization, Kinetic and Thermodynamic Calculations using Spartan Software - A Review. *Archives of Organic and Inorganic Chemical Sciences.*, 1(5), 122-125. http://doi.org/10.32474/AOICS.2018.01.000123

Reinke, L., Koch, M., Müller-Renno, C., & Kubik, S. (2021). Selective sensing of adenosine monophosphate (AMP) over adenosine diphosphate (ADP), adenosine triphosphate (ATP), and inorganic phosphates with zinc(ii)-dipicolylamine-containing gold nanoparticles., *Organic & Biomolecular Chemistry*, 19, 3893. https://doi.org/10.1039/d1ob00341k

Rubio, J., Martí-Centelles, V., Burguete, M. I., & Luis, S. V. (2013). Synthesis and organogelating ability of bis-urea pseudopeptidic compounds, *Tetrahedron*, 69, 2302-2308. https://doi.org/10.1016/j.tet.2013.01.007

Valls, A, Burguete, M.I., Kuret, L., Altava, B., & Luis, S. V. (2022). Open chain pseudopeptides as hydrogelators with reversible and dynamic responsiveness to pH, temperature and sonication as vehicles for controlled drug delivery., *J. Mol. Liquids*, 348, 118051. https://doi.org/10.1016/j.molliq.2021.118051

Verdejo, B., Ferrer, A., Blasco, S., Castillo, C. E., González, J., Latorre, J., Máñez, M.A., García Basallote, M., Soriano, C., & García-España, E. (2007). Hydrogen and Copper Ion-Induced Molecular Reorganizations in Scorpionand-like Ligands. A Potentiometric, Mechanistic, and Solid-State Study., *Inorganic Chemistry*, 46, 5707-5719. https://doi.org/10.1021/ic700643n

Yang, Y., Hao, S., Lei, X., Chen, J., Fang, G., Liu, J., Wang, S., & He, X. (2022). Design of metalloenzyme mimics based on self-assembled peptides for organophosphorus pesticides detection., *J. Hazardous Materials.*, 428, 128262. https://doi.org/10.1016/j.jhazmat.2022.128262